

# Geometry and Topology of Deep Neural Networks' Decision Boundaries

Bo Liu

College of Computer Science, Faculty of Information Technology  
Beijing University of Technology, Beijing, China  
liubo@bjut.edu.cn

## Abstract

Geometry and topology of decision regions are closely related with classification performance and robustness against adversarial attacks. In this paper, we use differential geometry and topology to explore theoretically the geometrical and topological properties of decision regions produced by deep neural networks (DNNs). The goals are to obtain some geometrical and topological properties of decision regions for given DNN models, and provide some principled guidances to designing and regularizing DNNs. At first, we give the curvatures of decision boundaries in terms of network weights. Based on the rotation index theorem and Gauss-Bonnet-Chern theorem, we then propose methods to identify the closeness and connectivity of given decision boundaries, and obtain the Euler characteristics of closed ones, all without the need to solve decision boundaries explicitly. Finally, we give necessary conditions on network architectures in order to produce closed decision boundaries, and sufficient conditions on network weights for producing zero curvature (flat or developable) decision boundaries.

## 1 Introduction

Although deep learning has been successfully applied to various domains including computer vision, speech recognition and natural language processing, the theoretical understanding of its success is still limited. One important theoretical aspect of deep learning is the geometry and topology of decision regions produced by DNNs. Geometry of decision boundaries concerns their curvature, area and convexity etc., while topology of decision boundaries considers their connectivity, openness and genus (the number of holes) etc. There are two important related questions: on one hand, how to obtain the geometrical and topological properties of decision boundaries for given DNN models? and on the other hand, what are the constraints on network architectures and weights in order to produce decision boundaries with certain geometrical and topological features? Besides

theoretical interests, answering these questions is also important to model selection [17, 39], reducing overfitting [5] and improving DNNs' robustness against adversarial attacks [33, 10]. Moreover, researches on the geometry and topology of decision regions will provide some principled guidances to network design, such as particular choices of network architectures to produce disconnected or closed decision boundaries, and regularizing curvature or number of connected components to boost robustness or accuracy.

Researches on the geometry and topology of DNN produced decision regions are still at their infancy. This paper aims at exploring the geometrical and topological structures of DNNs' decision regions with knowledges from differential geometry and topology [4, 25]. We first use differential geometry to compute the curvatures of decision boundaries. We then use global differential geometry, which establishes the analytical connection between local curvature and global topology of manifolds, to identify some topological properties of decision boundaries. Meanwhile, we formulate geometrical and topological properties in terms of network architecture and weights, and based on which it is possible to design DNNs with desired properties.

The contributions of this paper are summarized as follows:

- The curvatures of decision boundaries in terms of network parameters are given for 2d, 3d and higher-dimensional inputs respectively, using knowledges of differential geometry.
- Based on global differential geometry, more specifically, rotation index theorem for curves and Gauss-Bonnet-Chern theorem for 2d surfaces and higher-dimensional manifolds, we propose methods to identify the closeness and connectivity of given decision boundaries, and compute the Euler characteristics of closed ones, without the need to solve them explicitly.
- We give necessary conditions on network architectures for producing closed decision boundaries.
- For DNNs with any input dimension, we give sufficient conditions on network weights in order to produce zero curvature (flat or developable) decision boundaries.

This paper is organized as follows. Section 1.1 is related work. In section 2, we present the preliminaries of differential geometry and topology, and introduce the feed-forward deep neural network models, as well as some definitions and notations. Computations of curvatures of decision boundaries for 2d, 3d and higher-dimensional input spaces are explored in section 3. In section 4, we propose methods to identify the topological properties of decision boundaries, including Euler characteristic, openness and connectivity. Section 5 gives the necessary conditions on network architecture for producing closed decision boundaries. Section 6 presents the sufficient conditions for zero curvature decision boundaries. Finally, we give our conclusion and future work. The detailed proofs of main results are given in section 7.

## 1.1 Related work

**Geometry and topology of DNN produced decision regions** There have been some works on the geometry and topology of DNN produced decision regions. [38] experimentally finds that the decision boundary can become exponentially curved with depth, thus enabling highly complex classifications. [33, 10] show that decision boundaries exhibiting quasi-linear behavior in the vicinity of data points can improve adversarial robustness. Although numerical computations of curvatures have been presented in these works, systematic expressions of curvatures in terms of network weights are still missing. [10] demonstrates that the decision regions of CaffeNet [20] trained on ImageNet are connected. Based on persistent homology [9], [39, 17] compute the topological properties of DNNs decision boundaries by constructing simplicial complexes of decision boundaries with discrete data points. On the contrary, our methods are analytical and based on global differential geometry. [35] demonstrates that a sufficiently wide hidden layer is necessary to produce disconnected decision regions. [2] shows that the decision regions are open for DNNs with width less than or equal to input dimensions. [3] shows the topological expressiveness advantage of deep networks over shallow ones in terms of bounds on the sum of Betti numbers. To achieve a better balance between accuracy and overfitting, [5, 19] propose persistent homology based connectivity regularizers for logistic regression classifier and autoencoder respectively.

**Loss landscape of DNNs** In the field of deep learning theory, the loss landscape of DNNs is closely related to geometry and topology. There have been many works on the landscapes of various deep learning related models. Most of them focus on the existence of spurious local minima, where local search based optimization methods (such as the commonly used gradient descent) can easily get stuck.

It has been shown that there are no spurious local minima or spurious valleys for some specific types of networks, including deep linear networks [21, 32, 23, 46, 37, 48], one-hidden-layer networks with quadratic activation function [42, 8], very wide networks [45, 34, 26, 36, 6], deep linear residual networks [18], and networks with special type of extra neurons [28, 29, 22] and specially designed networks [15, 13, 11].

For ReLU networks, however, spurious local minima are common as evidenced in the studies of e.g., [41, 44, 49, 47]. [24] shows that ReLU networks with hinge loss can only have non-differentiable local minima. [40] shows that by Gaussian weight initialization, there is a high probability of initializing in a basin with small minimal loss for over-parameterized one-hidden-layer ReLU networks. [43] exhibits that for Gaussian input, the volume of differentiable regions containing sub-optimal local minima is exponentially vanishing for one-hidden-layer ReLU networks. [31] gives the conditions for the existence of non-differentiable local minima and saddle points for one-hidden-layer ReLU networks, and shows that the probability of existing spurious local minima is exponentially vanishing in regions where data points are not too scarce.

Besides theoretical researches on loss landscape, there have been some experimental explorations on landscape visualization [16, 30, 27], geometry of level sets [12] and mode connectivity [7, 14].

[1] presents an algorithm to compute the topological features of neural networks objective functions.

## 2 Preliminaries

### 2.1 Fully-connected feed-forward deep neural networks

We consider in this paper fully-connected feed-forward deep neural networks for binary classification. Let  $d$  be the input dimension,  $L$  be the number of layers and  $d_i$  be the width of layer  $i$  with  $d_0 = d$ . There is a single output,

$$f(\mathbf{x}) = \mathbf{a}^T \sigma(\mathbf{W}^L \sigma(\mathbf{W}^{L-1} \dots \sigma(\mathbf{W}^1 \mathbf{x} + \mathbf{b}^1) + \dots + \mathbf{b}^{L-1}) + \mathbf{b}^L) + c, \quad (1)$$

where  $\mathbf{x} \in \mathbb{R}^d$  is the input,  $\mathbf{W}^i \in \mathbb{R}^{d_i \times d_{i-1}}$  and  $\mathbf{b}^i \in \mathbb{R}^{d_i}$  are the weight matrix and bias vector of layer  $i$  respectively,  $\mathbf{a} \in \mathbb{R}^{d_L}$  and  $c$  are the weight vector and bias of the output layer.  $\sigma: \mathbb{R} \rightarrow \mathbb{R}$  is the activation function of every hidden layer which applies component-wise. We consider in this paper activation functions that are continuous and strictly monotonically increasing (thus bijective), including the commonly used sigmoid, leaky ReLU ( $\sigma(t) = \max\{t, \alpha t\}$  for  $0 < \alpha < 1$ ) and softplus ( $\sigma(t) = \frac{1}{\alpha} \log(1 + e^{\alpha t})$ ) which can approximate ReLU activation arbitrarily well.

For binary classification, the solution to  $f(\mathbf{x}) = 0$  gives the decision boundary,  $f(\mathbf{x}) > 0$  gives the decision region of positive class and  $f(\mathbf{x}) < 0$  specifies the decision region of negative class.

The pre-image of a mapping  $f: U \rightarrow V$  is defined as the set  $\{x \in U | f(x) \in V\}$ .  $[d]$  stands for  $\{1, 2, \dots, d\}$ . Both  $\mathbf{w}_i$  and  $W_{i,\cdot}$  represent the  $i$ th row of matrix  $\mathbf{W}$ , and  $W_{\cdot,i}$  denotes the  $i$ th column of  $\mathbf{W}$ .

### 2.2 Differential geometry and topology

In this subsection, we will give a brief introduction to the concepts and knowledges of differential geometry and topology that will be used later in this paper. Interested readers are referred to [4, 25] for the details.

#### 2.2.1 Differential geometry of curves

A planar curve is parameterized as  $\mathbf{r}(t) = \begin{pmatrix} x(t) \\ y(t) \end{pmatrix}$ , which maps the parameter  $t \in \mathbb{R}$  to a point  $\mathbf{r}(t) \in \mathbb{R}^2$  on the curve. Arc length  $s$  is usually used as the parameter  $t$ . The tangent vector at a point on the curve is defined as  $\mathbf{T} = \frac{d\mathbf{r}(s)}{ds}$ . The Frenet formula  $\frac{d\mathbf{T}(s)}{ds} = k_r \mathbf{N}_r$  gives the definition of planar curvature  $k_r$ , where  $\mathbf{N}_r$  is the unit normal vector.

For a closed planar curve  $C$  with counter-clockwise positive direction and without self-intersections, the rotation index theorem states  $\frac{1}{2\pi} \int_C k_r ds = 1$ , whose intuitive meaning is when moving along the closed curve for one cycle, the tangent vector will rotate just  $2\pi$ .

### 2.2.2 Differential geometry of surfaces

A 2d surface is locally parameterized as  $\mathbf{r}(u, v) = (x(u, v), y(u, v), z(u, v))^T$ , which maps the parameters  $(u, v) \in \mathbb{R}^2$  to a point  $\mathbf{r}(u, v) \in \mathbb{R}^3$  on the surface. Let  $ds$  be the infinitesimal arc length, then  $ds^2 = d\mathbf{r} \cdot d\mathbf{r} = Edu^2 + 2Fdudv + Gdv^2$ , where  $E = \mathbf{r}_u \cdot \mathbf{r}_u$ ,  $F = \mathbf{r}_u \cdot \mathbf{r}_v$ ,  $G = \mathbf{r}_v \cdot \mathbf{r}_v$  are called coefficients of the first fundamental form.  $\mathbf{r}_u$  denotes  $\frac{\partial \mathbf{r}(u, v)}{\partial u}$ . The second fundamental form, which measures the distance from  $\mathbf{r}(u + du, v + dv)$  to the tangent plane at  $\mathbf{r}(u, v)$ , is given as  $Ldu^2 + 2Mdudv + Ndv^2$ , where  $L = \mathbf{r}_{uu} \cdot \mathbf{n}$ ,  $N = \mathbf{r}_{vv} \cdot \mathbf{n}$ ,  $M = \mathbf{r}_{uv} \cdot \mathbf{n}$  are called coefficients of the second fundamental form.  $\mathbf{n} := \frac{\mathbf{r}_u \times \mathbf{r}_v}{|\mathbf{r}_u \times \mathbf{r}_v|}$  is the unit normal vector.

At each point on the surface, there are two principal curvatures  $k_1$  and  $k_2$  defined along two orthogonal principal directions. The total curvature (or Gaussian curvature) is defined as  $K = k_1 k_2 = \frac{LN - M^2}{EG - F^2}$ .

The classification theorem of compact surfaces states that all orientable 2d compact surfaces can be classified into topologically equivalent groups by their Euler characteristics. The Euler characteristic  $\chi(S)$  of a 2d closed surface  $S$  can only take a value in  $\{2, 0, -2, \dots, -2n, \dots\}$ . For example,  $\chi = 2$  for sphere,  $\chi = 0$  for torus and  $\chi = -2$  for double torus.  $n = \frac{2 - \chi(S)}{2}$  is called the genus of  $S$ , i.e., the number of holes in  $S$ .

For an orientable 2d compact surface  $S$ , the Gauss-Bonnet theorem states  $\iint_S K d\sigma = 2\pi\chi(S)$ , where  $d\sigma$  is the area element. Gauss-Bonnet theorem establishes the connection between local curvature and global topological property.

### 2.2.3 Differential geometry of higher-dimensional manifolds

High-dimensional case is much complex and abstract. A  $k$ -dimensional manifold is locally parameterized as  $\mathbf{r} = \mathbf{r}(x_1, x_2, \dots, x_k)$ . Then

$$ds^2 = d\mathbf{r} \cdot d\mathbf{r} = \sum_{ij=1}^k g_{ij} dx_i dx_j$$

where  $g_{ij} = \mathbf{r}_i \cdot \mathbf{r}_j$ .  $g = (g_{ij})$  is called metric tensor. The Riemannian connection is defined as  $\Gamma_{ik}^m := \frac{1}{2} \sum_j g^{mj} (\partial_k g_{ij} + \partial_i g_{kj} - \partial_j g_{ik})$ , where  $g^{mj}$  is the element of  $g^{-1}$ , the inverse matrix of  $g$ .

The Riemann curvature tensor is defined as

$$R_{bik}^a := \Gamma_{kb,i}^a - \Gamma_{ib,k}^a + \sum_c \Gamma_{ic}^a \Gamma_{kb}^c - \sum_c \Gamma_{kc}^a \Gamma_{ib}^c$$

At each point on the manifold, the curvature along any 2d tangent subspace (like  $K$  for 2d surfaces) can be obtained from  $R_{bik}^a$ . The curvature 2-form is defined as

$$\Omega_{ab} = \frac{1}{2} \sum_{i,k} R_{abik} dx^i \wedge dx^k = \frac{1}{2} \sum_{i,k,c} g_{ac} R_{bik}^c dx^i \wedge dx^k,$$

where  $\wedge$  is the outer product of differential forms.

The Euler characteristic  $\chi(M)$  of a manifold  $M$  is defined as the signed sum of its Betti numbers, which in turn is a concept from algebraic topology. Intuitively, the 1st Betti number  $b_0$  is the number of connected components, and the  $i$ th Betti number  $b_i$  ( $i \geq 1$ ) counts the number of  $(i + 1)$ -dimensional holes of the manifold.

The Gauss-Bonnet-Chern theorem for high-dimensional orientable compact manifolds gives the relationship between local curvature and global topological property. For a  $2n$ -dimensional orientable compact manifold  $M$ , Gauss-Bonnet-Chern theorem states

$$\chi(M) = \int_M e(M),$$

where  $e(M) = \frac{1}{2^n (2\pi)^{n!}} \sum_{a_1, a_2, \dots, a_{2n}} \varepsilon_{a_1, a_2, \dots, a_{2n}} \Omega^{a_1 a_2} \wedge \dots \wedge \Omega^{a_{2n-1} a_{2n}}$ ,  $\Omega^{ab} = \Sigma_{c,d} g^{ac} g^{bd} \Omega_{cd}$ ,  $\varepsilon_{a_1 \dots, a_{2n}} = \sqrt{\det(g)} \delta_{a_1 \dots a_{2n}}^{1 \dots 2n}$ .  $\delta_{a_1 \dots a_{2n}}^{1 \dots 2n}$  is the generalized Kronecker symbol which equals 1 if  $a_1, \dots, a_{2n}$  is an even permutation of  $1, 2, \dots, 2n$ ;  $-1$  if odd permutation, and 0 otherwise.

### 3 Curvature of decision boundary

While there are numerical computations of curvatures in [38, 33], a systematic and analytical treatment of decision boundary's curvature in the framework of differential geometry is still absent. In this section, we will compute the curvature of decision boundaries for 2d, 3d and higher-dimensional input spaces respectively. The key observation is that although usually the decision boundaries cannot be solved analytically, we can use the equation  $f(\mathbf{x}) = 0$  to describe them implicitly and use derivatives of implicit functions to compute curvatures. The expressions of curvatures obtained in this section will be used frequently later in this paper.

#### 3.1 2D input space

In 2d input space, the decision boundary is in general a curve, either open or closed, and satisfy  $f(x, y) = 0$ . This gives an implicit function  $y = y(x)$ . We will use the Frenet formula for planar curves to compute the curvature of decision boundaries in 2d.

**Lemma 3.1.** *The planar curvature of a decision boundary in 2d input space is*

$$k_r = - \frac{f_{xx} f_y^2 - 2f_x f_y f_{yx} + f_x^2 f_{yy}}{f_y^3} \left( 1 + \frac{f_x^2}{f_y^2} \right)^{\frac{3}{2}}, \quad (2)$$

where  $f = f(x, y)$  is the output function of neural network,  $f_x = \frac{\partial f}{\partial x}$  and so on.

For neural networks, we can compute the derivatives involved in (2) and consequently  $k_r$ . As an example, here we give the derivatives of one-hidden-layer networks. More expressions of curvatures in terms of network weights will be given in section 7. For one-hidden-layer network  $f(\mathbf{x}) = \mathbf{a}^T \sigma(\mathbf{W}\mathbf{x} + \mathbf{b}) + c$ , its 1st-order and 2nd-order partial derivatives are as follows,

$$\begin{aligned} f_x &= \sum_i a_i \sigma'_i W_{i1}, & f_y &= \sum_i a_i \sigma'_i W_{i2} \\ f_{xx} &= \sum_i a_i \sigma''_i W_{i1} W_{i1}, & f_{yx} &= \sum_i a_i \sigma''_i W_{i1} W_{i2} \\ f_{xy} &= \sum_i a_i \sigma''_i W_{i1} W_{i2}, & f_{yy} &= \sum_i a_i \sigma''_i W_{i2} W_{i2}, \end{aligned} \quad (3)$$

where  $\sigma'_i = \sigma'(\mathbf{w}_i \cdot \mathbf{x} + \mathbf{b}_i)$ ,  $\sigma''_i = \sigma''(\mathbf{w}_i \cdot \mathbf{x} + \mathbf{b}_i)$ .

### 3.2 3D input space

In 3d input space, the decision boundary is a 2d surface satisfying  $f(x, y, z) = 0$ . Its Gaussian curvature is described by the following lemma.

**Lemma 3.2.** *The Gaussian curvature of a decision boundary in 3d input space is*

$$\begin{aligned} K &= [(2f_x f_z f_{xz} - f_{xx} f_z^2 - f_{zz} f_x^2) (2f_y f_z f_{yz} - f_{yy} f_z^2 - f_{zz} f_y^2) - \\ & (f_x f_z f_{yz} + f_y f_z f_{xz} - f_x f_y f_{zz} - f_{xy} f_z^2)^2] / [f_z^2 (f_x^2 + f_y^2 + f_z^2)^2] \end{aligned} \quad (4)$$

### 3.3 Higher-dimensional input space

For high-dimensional case, we need to compute the curvature tensor and curvature 2-form. Before that, it is necessary to compute metric tensor  $g_{ij}$  and Riemannian connection  $\Gamma_{ik}^m$ . The details of computation will be presented in subsection 7.3.

## 4 Topology of decision boundary

In this section, based on the rotation index theorem for planar curves and Gauss-Bonnet-Chern theorem for surfaces and higher-dimensional manifolds, we describe how to judge whether a decision boundary is open or closed, connected or disconnected, and how to obtain the Euler characteristic of a closed boundary. We will utilize the following assumption in our proofs.

**Assumption 4.1.** *The domain of definition for input data is a  $d$ -dimensional box, that is,  $x_i \in [x_{i_{min}}, x_{i_{max}}]$  ( $\forall i \in [d]$ ).  $x_{i_{min}}$  and  $x_{i_{max}}$  can be infinite.*

This assumption is reasonable for commonly used practical data, such as image pixels taking values in  $[0, 255]$ .

### 4.1 2D input space

The following theorem can be used to judge the openness of a decision boundary in 2d input space.

**Theorem 4.1.** *In 2d input space, a single-component decision boundary without self-intersections is closed if and only if*

$$I_{2d} := -\frac{1}{2\pi} \iint_D \text{sgn}(f(x, y)) \frac{\partial \left( k_r \sqrt{1 + f_x^2/f_y^2} \right)}{\partial y} dx dy = 1 \quad (5)$$

holds, where  $k_r$  is the curvature of decision boundary curve given in (2),  $\text{sgn}(x)$  is the sign function which equals 1 when  $x > 0$  and 0 otherwise.  $D$  is input's definition domain.

**Remark:** 1) For the integral in theorem 4.1,  $k_r, f_x, f_y$  are functions of  $x, y$ . Therefore, this integral is clearly defined and there is no need to solve the decision boundary curve explicitly which is usually a hard task. 2) Although openness is a global topological property,  $k_r(x, y)$  etc. are local quantities, thanks to the rotation index theorem, we can determine global topology via integral of these local quantities. This local-global relationship will be seen in 3d and higher-dimensional inputs as well. 3) calculating the integral appeared in (5) can be fulfilled by numerical techniques. Concrete numerical computation of this integral and analysis of its accuracy are leaved to our future work. Here we give a simple example. For a one-hidden-layer network  $f(\mathbf{x}) = \mathbf{a}^T \sigma(\mathbf{W}\mathbf{x} + \mathbf{b}) + c$  with one-hot vector  $\mathbf{a}$  (i.e., only one component of  $\mathbf{a}$  is non-zero), one can verify using (2) and (3) that  $k_r(x, y) = 0$ , hence  $I_{2d} = 0$  and the decision boundary is open by theorem 4.1. In subsection 6.1, we will show that one-hot vector  $\mathbf{a}$  actually produces linear decision boundaries, for which  $I_{2d} = 0$  truly holds (see (21) in subsection 7.4). 4) Since  $\sigma$  is bijective, no self-intersections will be created in the decision boundary curve, hence the corresponding prerequisite of theorem 4.1 is satisfied for DNNs.

Having theorem 1, we can proceed to analyze whether a decision region is connected or not, and the number of components in it if disconnected. The results are summarized in the following theorem.

**Theorem 4.2.** *For 2d input space, if  $I_{2d} = n$  (a positive integer), then the decision region of positive class has  $n$  closed components. Otherwise ( $I_{2d} \neq n$ ), at least one component of the decision region of positive class is open.*

Theorem 4.2 implies immediately the following corollary.

**Corollary 4.1.** *If  $I_{2d} = n$  (a positive integer) and  $n > 1$ , then the decision region of positive class is disconnected, otherwise ( $I_{2d} = 1$ ) it is connected.*

**Remark.** 1) Theorem 4.2 tells us that if  $I_{2d} \neq n$  there must be open components. However, it does not specify the number of open components. For an open component  $D_i$ , we have (the proof is deferred to subsection 7.4)

$$0 < -\frac{1}{2\pi} \iint_{D_i} \frac{\partial \left( k_r \sqrt{1 + f_x^2/f_y^2} \right)}{\partial y} dx dy < 1,$$



which indicates that it is not enough by the value of

$$I_{2d} = \Sigma_i - \frac{1}{2\pi} \iint_{D_i} \frac{\partial \left( k_r \sqrt{1 + f_x^2/f_y^2} \right)}{\partial y} dx dy$$

alone to identify the number of open components. 2) Corollary 4.1 gives the condition for the existence of disconnected decision regions. [35] shows that a sufficiently wide hidden layer is necessary to produce disconnected decision regions, while corollary 4.1 shows that  $I_{2d} = n$  and  $n > 1$  (which constrains the network weights) are also necessary to have disconnected decision regions. Therefore, our result in corollary 4.1 extends the conclusion in [35] which only provides architectural constraint.

## 4.2 3D input space

In this subsection, we discuss how to identify whether the decision surface in 3d input space for a trained model is open or closed, connected or disconnected, and how to find the genus of single-component closed decision surfaces. First, we establish the following theorem to judge the openness of a decision surface.

**Theorem 4.3.** *In 3d input space, a single-component decision boundary is closed if and only if*

$$I_{3d} := \iiint_D \text{sgn}(f(x, y, z)) \frac{\partial \left( K \sqrt{f_x^2 + f_y^2 + f_z^2/f_z} \right)}{\partial z} dV = 2\pi\chi, \quad (6)$$

where  $D$  is domain of definition for input,  $\chi$  takes a value in  $\{2, 0, -2, \dots, -2n, \dots\}$ .

Based on theorem 4.3, the connectivity and Euler characteristic of a decision surface are given in the following theorem.

**Theorem 4.4.** *For a closed decision surface  $S$  in 3d input space, if  $I_{3d} = 2\pi\chi$  and  $\chi$  is a even number, then all components of  $S$  are closed; otherwise, at least one component of  $S$  is open. If  $\frac{I_{3d}}{2\pi} = 2n$ , ( $n$  is a positive integer and  $n \geq 2$ ), then  $S$  is disconnected and has at least two sphere-like components. Finally, if  $S$  is closed and has only one component, its Euler characteristic is  $\chi(S) = \frac{I_{3d}}{2\pi}$ .*

**Remark.** If  $\frac{I_{3d}}{2\pi} = 2n$  ( $n$  is an arbitrary integer) and there are more than one closed components in  $S$ , we cannot uniquely determine by  $I_{3d}$  alone the number of connected components and their topological types. For example, a torus has  $\chi = 0$ , and a surface composed of a sphere and a double-torus also produces  $\sum \chi = 2 - 2 = 0$ .

## 4.3 Higher-dimensional input space

For higher-dimensional input space, the topological structure of a closed orientable decision boundary can be characterized by its Euler characteristic. The following theorem shows that the Euler characteristic of a DNN's decision boundary can be obtained by an integral of a curvature related quantity.

**Theorem 4.5.** For a  $2n$ -dimensional closed decision boundary manifold  $M$ , its Euler characteristic  $\chi(M)$  can be obtained by

$$\chi(M) = \int_D \text{sgn}(f(\mathbf{x})) d\mathbf{e} \quad (7)$$

where

$$e = \frac{1}{2^n (2\pi)^n n!} \sum_{a_1, a_2, \dots, a_{2n}} \varepsilon_{a_1, a_2, \dots, a_{2n}} \Omega^{a_1 a_2} \wedge \dots \wedge \Omega^{a_{2n-1} a_{2n}}, \quad (8)$$

and  $\Omega^{ab} = \sum_{c,d} g^{ac} g^{bd} \Omega_{cd}$ ,  $\varepsilon_{a_1, a_2, \dots, a_{2n}} = \sqrt{\det(g)} \delta_{a_1 \dots a_{2n}}^{1 \dots 2n}$ .  $D$  is input's definition domain. The expression of  $\Omega_{ab}$  will be given in subsection 7.3.

**Remark.** For high dimensional input space, computing the integral in (7) faces two difficulties: the exponentially increasing number of terms in  $e$ , and high dimensions of the integral. Efficient computation of this integral using techniques such as sampling will be one of our future work.

## 5 Conditions for producing closed decision boundaries

In section 4, we have considered how to identify the closeness of decision boundaries of trained models. In this section, we want to probe the following related problem: what are the architectural constraints on DNNs in order to produce closed boundaries? This problem is answered by the following theorem.

**Theorem 5.1.** Form deep neural networks with continuous and bijective activation function, in order to produce closed decision boundaries, the width of the last hidden layer must satisfy  $d_L > d$ , and the width of any other intermediate layer must satisfy  $d_l \geq d$ .

**Remark.** 1) When  $d_L > d$ , decision boundary is geometrically the intersection of the hyperplane defined by  $\mathbf{a}^T \mathbf{O}_L + c = 0$ , ( $\mathbf{O}_L \in \mathbb{R}^{d_L}$ ) with the curved hypersurface formed by  $\sigma(W^L \sigma(W^{L-1} \dots \sigma(W^1 \mathbf{x} + \mathbf{b}^1) + \dots + \mathbf{b}^{L-1}) + \mathbf{b}^L)$ . An illustrative example for 2d input space is shown in fig. 1.

2) Theorem 5.1 gives the necessary conditions for DNNs to produce closed decision boundaries. However, these conditions are not sufficient, and there are weights constraints as well in order to create closed decision boundaries. At first, the transformations induced by weights  $(W^l)_{l=1}^L$  should not cause the decision boundaries to collapse. Therefore, weights  $(W^l)_{l=1}^L$  need to have full rank if  $d_l = d$  for  $l = 1, 2, \dots, L-1$ . Next, as shown in section 4, there are constraints on the indexes  $I_{2d}$  and  $I_{3d}$  etc. (which depend on weights) in order to produce closed decision boundaries. Here we give a counter-example to show that even the architectural constraints are satisfied, particular choice of weights can still produce open decision boundaries. For a one-hidden-layer network with

sigmoid activation and 2d input, assume  $\mathbf{W} = \begin{pmatrix} 0 & 0 \\ 1 & 0 \\ 0 & 1 \end{pmatrix}$ ,  $\mathbf{b} = \begin{pmatrix} 0 \\ 0 \\ 0 \end{pmatrix}$ , and

$\mathbf{a} = \left(0, \frac{1}{\sqrt{2}}, \frac{1}{\sqrt{2}}\right)^T$ ,  $c = -1$ . The image of  $\mathbf{W}\mathbf{x} + \mathbf{b}$  ( $\mathbf{x} \in \mathbb{R}^2$ ) will be the  $y-z$  plane in  $\mathbb{R}^3$ .  $\mathbf{a}$  and  $c$  determine a plane  $p$  by  $\mathbf{a}^T \mathbf{O} + c = 0$ . The normal of  $p$  has no  $x$  component since  $a_1 = 0$ .  $\sigma^{-1}(p)$  is a developable surface and the normal at any point on this surface has no  $x$  component as well, and this surface is not closed due to  $\sigma^{-1}$  is bijective. Therefore, the intersection of  $\mathbf{W}\mathbf{x} + \mathbf{b}$  (i.e., the  $y-z$  plane) with  $\sigma^{-1}(p)$  is a curve that is not closed, demonstrating that no closed decision boundary is generated.

3) Comparing with [2], which concludes that if the widths of all hidden layers are less than or equal to the input dimension then the decision regions will be open, our results in Theorem 5.1 explicitly requires  $d_L > d$  to produce closed decision regions, thus our results are more informative. We also discuss the constraints on weights as in the previous remark.

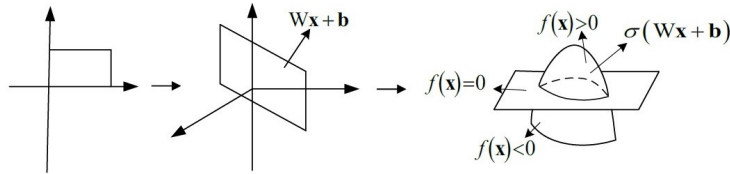


Figure 1: Intersection of  $\sigma(\mathbf{W}\mathbf{x} + \mathbf{b})$  with hyperplane  $\mathbf{a}^T \mathbf{O} + c = 0$  produces a closed decision boundary.

## 6 Conditions on network weights for zero curvature decision boundaries and the geometric interpretations

Given the expressions of decision boundaries' curvatures in section 3, one way wonder what network architectures and weights can generate decision boundaries with desired geometrical properties, such as flatness, convexity etc. As a starting point, we discuss in this paper how to get zero curvature (flat or developable along some directions) decision boundaries with appropriate network weights. It has been shown in [33] that there is a strong relation between small curvature decision boundaries and large robustness against adversarial attacks.

We will start with low-dimensional input space and networks with one or two hidden layers, and then extend to the general case of any input dimension and DNNs. We will derive the sufficient conditions for zero curvatures, and give

the geometric interpretations of some conditions to show intuitively how the flat or developable boundaries are produced.

## 6.1 2D input space and one-hidden-layer networks

In 2D input space, the zero curvature decision boundary is a line. The sufficient conditions for 2d input space and one-hidden-layer networks are given by the following theorem.

**Theorem 6.1.** *For one-hidden-layer neural networks  $f(x) = \mathbf{a}^T \sigma(W\mathbf{x} + \mathbf{b}) + c$  ( $\mathbf{a} \in \mathbb{R}^{d_1}$ ) with 2d input  $\mathbf{x}$  and bijective and continuous activation function  $\sigma$ , one of the following conditions is sufficient to produce linear decision boundaries with zero curvatures: for  $i, j \in [d_1]$ ,*

- a)  $a_i W_{i1} = 0$  or  $a_i W_{i2} = 0$ .
- b)  $a_i a_j (W_{i1} W_{j2} - W_{i2} W_{j1}) = 0$ . A special case is that  $\mathbf{a}$  is a one-hot vector, i.e., only one component of  $\mathbf{a}$  is non-zero.

$a_i W_{i1} = 0$  or  $a_i W_{i2} = 0$  means if  $a_i \neq 0$ ,  $W_{i1} = 0$  or  $W_{i2} = 0$ . Consequently, if  $\forall i, a_i \neq 0$ , we have  $W_{\cdot,1} = 0$  or  $W_{\cdot,2} = 0$ . Geometrically,  $W_{\cdot,1} = 0$  or  $W_{\cdot,2} = 0$  transforms the 2d input space into a line which, after activation by  $\sigma$ , results in a curve. This curve will intersect the plane (or line) in  $\mathbb{R}^{d_1}$  specified by  $\mathbf{a}$  and  $c$  at a point, whose pre-image in input space is a line. Thus,  $W_{\cdot,1} = 0$  or  $W_{\cdot,2} = 0$  produces linear decision boundaries. Fig.2(a) illustrates the case of  $W_{\cdot,1} = 0$ .

If  $a_i \neq 0$  and  $W_{i1} = 0$  or  $W_{i2} = 0$  for some values of  $i$ , for example, if  $d_1 = 3$  and  $\mathbf{a} = (0, 1, 1)^T$ ,  $W_{21} = W_{31} = 0$ , then the image of  $W\mathbf{x} + \mathbf{b} = \begin{pmatrix} W_{11}x + W_{12}y \\ W_{22}y \\ W_{32}y \end{pmatrix} + \mathbf{b}$  is a plane  $p$  with normal  $\mathbf{n} = (0, W_{32}, -W_{22})^T$ . After activation by  $\sigma$ ,  $\sigma(p)$  becomes a curved surface whose normal's  $x$  component is also 0. The intersection of  $\sigma(p)$  with the plane  $q$  in  $\mathbb{R}^{d_1}$  with normal  $\mathbf{a}$  is a straight line parallel to  $x$  axis, whose pre-image in input space is a line parallel to  $x$  axis. This case is illustrated in fig.2(b).

The case of  $(W_{i1} W_{j2} - W_{i2} W_{j1}) = 0$  ( $\forall i, j \in [d_1]$ ) means  $W$  is rank-deficient and the image of  $W\mathbf{x} + \mathbf{b}$  is a line, similar to the case in fig. 2(a).

## 6.2 2D input space and two-hidden-layer networks

For this case, the sufficient conditions for linear decision boundaries are given as follows.

**Theorem 6.2.** *For two-hidden-layer networks  $f(\mathbf{x}) = \mathbf{a}^T \sigma(U\sigma(V\mathbf{x} + \mathbf{b}_1) + \mathbf{b}_2) + c$  ( $V \in \mathbb{R}^{d_1 \times 2}$ ,  $U \in \mathbb{R}^{d_2 \times d_1}$ ,  $\mathbf{a} \in \mathbb{R}^{d_2}$ ) with 2d input space and bijective and continuous activation function  $\sigma$ , one of the following conditions is sufficient to produce linear decision boundaries: for  $j, l \in [d_1]$ ,  $i \in [d_2]$ ,*

- a)  $V_{\cdot,1} = 0$  or  $V_{\cdot,2} = 0$  or  $V_{j1} V_{l2} - V_{j2} V_{l1} = 0$ .
- b)  $a_i U_{ij} V_{j1} = 0$  or  $a_i U_{ij} V_{j2} = 0$  or  $a_i U_{ij} (V_{j1} V_{l2} - V_{j2} V_{l1}) = 0$ .

Case a) only concerns weight  $V$  of the first hidden layer, which transforms the 2d input space into a line. In case b), the weights  $U, V$  and  $\mathbf{a}$  in different layers work together to produce linear decision boundaries.

### 6.3 3D input space and one-hidden-layer networks

For 3d input space and one-hidden-layer networks, the sufficient conditions for zero curvature decision boundaries are presented in the following theorem.

**Theorem 6.3.** *For one-hidden-layer networks  $f(\mathbf{x}) = \mathbf{a}^T \sigma(\mathbf{W}\mathbf{x} + \mathbf{b}) + c$  ( $\mathbf{W} \in \mathbb{R}^{d_1 \times 3}$ ) with 3d input and bijective and continuous activation function  $\sigma$ , any one of the following conditions is sufficient to produce decision boundaries with zero curvatures ( $K = 0$ ): for  $i, j \in [d_1]$ ,*

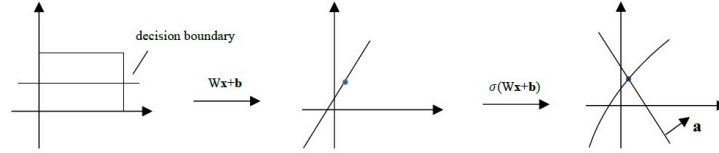
- a)  $a_i W_{i1} = 0$  or  $a_i W_{i2} = 0$  or  $a_i W_{i3} = 0$ .
- b)  $a_i a_j (W_{i2} W_{j3} - W_{i3} W_{j2}) = 0$ .

Fig. 2(c) illustrates the case of  $W_{i1} = 0$  for  $d_1 = 3$ . The 3d input space is mapped into a plane  $p$ . Denote by  $q$  the plane in  $\mathbb{R}^{d_1}$  determined by  $\mathbf{a}$  and  $c$ ,  $\sigma^{-1}(q)$  will be a curved surface. The intersection of  $p$  with  $\sigma^{-1}(q)$  is a curve, whose pre-image in input space is a developable surface that is curved along one direction and straight along the orthogonal direction (using the terms of differential geometry, one of the principal curvatures  $k_1$  and  $k_2$  is zero). It is worthy to point out that in 3d input space,  $K = k_1 k_2 = 0$  does not always imply planar decision boundaries ( $k_1 = k_2 = 0$ ), developable surfaces are also possible ( $k_1 = 0$  or  $k_2 = 0$ ) instead, as shown in fig. 2(c).

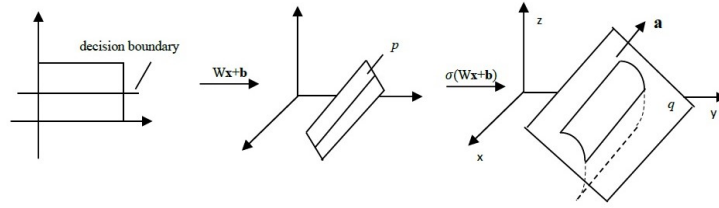
### 6.4 General case: higher dimensional input space and deep neural networks

It can be seen from the one-hidden-layer and two-hidden-layer networks (with either 2d or 3d input) discussed in previous subsections that, while deriving from different expressions of curvatures, there are some common conditions for zero curvature decision boundaries. By extension, we will give in this subsection the sufficient conditions for zero curvature decision boundaries for DNNs with arbitrary input dimensions. Our proof will be based on analyzing equation  $f(\mathbf{x}) = 0$  instead of complex curvature tensor. We shall point out that although flat decision boundaries can be obtained without utilizing the expressions of curvatures, many other geometry and topology related tasks, such as those in section 4, still rely heavily on curvatures.

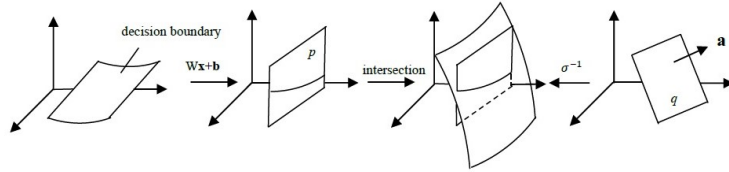
**Theorem 6.4.** *For fully-connected feed-forward deep neural networks  $f(\mathbf{x}) = \mathbf{a}^T \sigma(\mathbf{W}^L \sigma(\mathbf{W}^{L-1} \dots \sigma(\mathbf{W}^1 \mathbf{x} + \mathbf{b}^1) + \dots + \mathbf{b}^{L-1}) + \mathbf{b}^L) + c$ , the following conditions are sufficient to produce linear decision boundaries:  $a_i W_{ij}^L W_{jk}^{L-1} \dots W_{mn}^2 = 0$  ( $i, j, k, \dots, m, n$  are arbitrary) and vectors  $\mathbf{w}_l^1 = \mathbf{W}_l^1$ . ( $l \neq n$ ) are linear dependent. The following conditions are sufficient to produce decision boundaries that are straight along axis  $x_q$  :  $a_i W_{ij}^L W_{jk}^{L-1} \dots W_{mn}^2 = 0$  and  $W_{lq}^1 = 0$  ( $l \neq n$ ).*



(a) Rank-deficient  $W$  maps 2d input space into a line, and then the curve  $\sigma(W\mathbf{x} + \mathbf{b})$  intersects the line with normal  $\mathbf{a}$  at a point whose pre-image in input space is a linear decision boundary.



(b)  $W\mathbf{x} + \mathbf{b}$  maps 2d input space into a plane  $p$  in 3d, then the curved surface  $\sigma(p)$  intersects the plane  $q$  with normal  $\mathbf{a}$  at a line (both planes  $p$  and  $q$  are parallel to  $x$  axis) whose pre-image in input space is a linear decision boundary.



(c) Rank-deficient  $W$  maps 3d input space into a plane  $p$ , and its intersection with  $\sigma^{-1}(q)$  ( $q$  is the plane with normal  $\mathbf{a}$ ) is a curve whose pre-image in 3d input space is a developable surface decision boundary.

Figure 2: Illustrations of how decision boundaries with zero curvatures are generated.

**Remark:** We have obtained decision boundaries that are straight along certain axes. If one wants to have a decision boundary that is straight along an arbitrary direction, the input space can be rotated at first to make the desired direction be aligned with certain axis, then a decision boundary that is straight along this axis can be produced like before.

## 7 Proofs

### 7.1 Proof of Lemma 3.1

Using arc length  $s$  as parameter, a point on the decision boundary is represented as  $\mathbf{r} = \begin{pmatrix} x(s) \\ y(s) \end{pmatrix}$ . By  $ds = \sqrt{dx^2 + dy^2} = \sqrt{1 + y'^2}dx$ , we have

$\frac{dx}{ds} = \frac{1}{\sqrt{1+y'^2}}$ , where  $y' = \frac{dy}{dx}$ . The tangent vector  $\mathbf{T}(s)$  is

$$\mathbf{T}(s) := \frac{d\mathbf{r}}{ds} = \begin{pmatrix} \frac{dx}{ds} \\ \frac{dy}{dx} \frac{dx}{ds} \end{pmatrix} = \frac{1}{\sqrt{1+y'^2}} \begin{pmatrix} 1 \\ y' \end{pmatrix}.$$

The derivative of  $\mathbf{T}(s)$  is

$$\begin{aligned} \mathbf{T}' &= \frac{d^2\mathbf{r}}{ds^2} = \left(-\frac{1}{2}(1+y'^2)^{-\frac{3}{2}}\right) \cdot 2y'y'' \frac{dx}{ds} \begin{pmatrix} 1 \\ y' \end{pmatrix} + (1+y'^2)^{-\frac{1}{2}} \begin{pmatrix} 0 \\ y'' \cdot \frac{dx}{ds} \end{pmatrix} \\ &= \frac{y''}{(1+y'^2)^2} \begin{pmatrix} -y' \\ 1 \end{pmatrix} = \frac{y''}{(1+y'^2)^{\frac{3}{2}}} \begin{pmatrix} \frac{-y'}{\sqrt{1+y'^2}} \\ \frac{1}{\sqrt{1+y'^2}} \end{pmatrix}. \end{aligned}$$

Since  $\begin{pmatrix} \frac{-y'}{\sqrt{1+y'^2}} \\ \frac{1}{\sqrt{1+y'^2}} \end{pmatrix}$  is a unit vector, according to Frenet formula  $\mathbf{T}' = k_r \mathbf{N}_r$ , where  $\mathbf{N}_r$  is the unit normal vector, we get

$$k_r = y'' \cdot (1+y'^2)^{-\frac{3}{2}}. \quad (9)$$

We then need to compute  $y'$  and  $y''$  involved in (9). Given the equation of decision boundary  $f(x, y) = 0$  which implicitly defines a curve  $y = y(x)$ , its derivative with respect to  $x$  leads to

$$\frac{\partial f}{\partial x} + \frac{\partial f}{\partial y} \cdot \frac{dy}{dx} = 0$$

So  $y' = -\frac{f_x}{f_y}$  and consequently

$$y'' = -\frac{(f_{xx} + f_{xy}y')f_y - f_x(f_{yx} + f_{yy} \cdot y')}{f_y^2} = -\frac{f_{xx}f_y - 2f_xf_{yx} + \frac{f_x^2}{f_y}f_{yy}}{f_y^2}.$$

Substituting them into (9), we get (2). For convex decision boundary curves,  $y'' > 0$ . It then follows from (9) that  $k_r > 0$ , which is consistent with the conclusion of differential geometry for convex curves.

## 7.2 Proof of Lemma 3.2

In order to compute  $K$  at a point  $\mathbf{r} = (x, y, z)^T$  on the decision boundary, we need to compute  $E, F, G$  and  $L, M, N$ , i.e., the coefficients of the first and second fundamental forms, which in turn rely on the 1st-order and 2nd-order partial derivatives of  $\mathbf{r}$ . In the neighborhood around  $\mathbf{r}$ , we use  $(x, y)$  to parameterize the surface, thus  $(u, v) = (x, y)$ . The equation  $f(x, y, z) = 0$  defines a decision boundary surface  $z = z(x, y)$  implicitly. The 1st-order derivatives of  $\mathbf{r}$  are as follows.

$$\mathbf{r}_u = \frac{\partial \mathbf{r}}{\partial u} = \frac{\partial \mathbf{r}}{\partial x} = \left(1, 0, \frac{\partial z}{\partial x}\right)^T.$$

From  $f(x, y, z) = 0$ , we have  $\frac{\partial f}{\partial x} + \frac{\partial f}{\partial z} \cdot \frac{\partial z}{\partial x} = 0$ , thus  $\frac{\partial z}{\partial x} = -\frac{f_x}{f_z}$ . As a result,  $\mathbf{r}_u = \left(1, 0, -\frac{f_x}{f_z}\right)^T$ . Similarly,  $\mathbf{r}_v = \left(0, 1, -\frac{f_y}{f_z}\right)^T$ . The 2nd-order derivatives of  $\mathbf{r}$  are as follows.

$$\begin{aligned}\mathbf{r}_{uu} &= \frac{\partial^2 \mathbf{r}}{\partial x^2} = \left(0, 0, -\frac{(f_{xx} + f_{xz} \frac{\partial z}{\partial x}) f_z - f_x (f_{zx} + f_{zz} \frac{\partial z}{\partial x})}{f_z^2}\right)^T \\ &= \left(0, 0, \frac{2f_x f_z f_{xz} - f_{xx} f_z^2 - f_{zz} f_x^2}{f_z^3}\right)^T.\end{aligned}$$

Similarly, we can obtain

$$\mathbf{r}_{vv} = \left(0, 0, \frac{2f_y f_z f_{yz} - f_{yy} f_z^2 - f_{zz} f_y^2}{f_z^3}\right)^T.$$

and

$$\mathbf{r}_{uv} = \mathbf{r}_{vu} = \frac{\partial^2 \mathbf{r}}{\partial y \partial x} = \left(0, 0, -\frac{f_{xy} f_z^2 - f_y f_z f_{xz} - f_x f_z f_{yz} + f_x f_y f_{zz}}{f_z^3}\right)^T.$$

Then, the coefficients of the first fundamental form are:

$$E = \mathbf{r}_u \cdot \mathbf{r}_u = 1 + \frac{f_x^2}{f_z^2}, \quad F = \mathbf{r}_u \cdot \mathbf{r}_v = \frac{f_x f_y}{f_z^2}, \quad G = \mathbf{r}_v \cdot \mathbf{r}_v = 1 + \frac{f_y^2}{f_z^2}.$$

The unit normal vector at point  $\mathbf{r}$  is

$$\mathbf{n} := \frac{\mathbf{r}_u \times \mathbf{r}_v}{|\mathbf{r}_u \times \mathbf{r}_v|} = \frac{\left(\frac{f_x}{f_z}, \frac{f_y}{f_z}, 1\right)^T}{\sqrt{1 + \frac{f_x^2}{f_z^2} + \frac{f_y^2}{f_z^2}}} = \frac{(f_x, f_y, f_z)^T}{\sqrt{f_x^2 + f_y^2 + f_z^2}}.$$

The coefficients of the second fundamental form are

$$\begin{aligned}L = \mathbf{r}_{uu} \cdot \mathbf{n} &= \frac{2f_x f_z f_{xz} - f_{xx} f_z^2 - f_{zz} f_x^2}{f_z^2 \sqrt{f_x^2 + f_y^2 + f_z^2}} \\ N = \mathbf{r}_{vv} \cdot \mathbf{n} &= \frac{2f_y f_z f_{yz} - f_{yy} f_z^2 - f_{zz} f_y^2}{f_z^2 \sqrt{f_x^2 + f_y^2 + f_z^2}} \\ M = \mathbf{r}_{uv} \cdot \mathbf{n} &= \frac{f_x f_z f_{yz} + f_y f_z f_{xz} - f_x f_y f_{zz} - f_{xy} f_z^2}{f_z^2 \sqrt{f_x^2 + f_y^2 + f_z^2}}.\end{aligned}$$

Substituting the above expressions into Gaussian curvature  $K = \frac{LN - M^2}{EG - F^2}$  yields (4).



### 7.3 Curvatures for higher-dimensional input space

For high-dimensional input space, we need to compute the curvature tensor and curvature 2-form. Before that, the metric tensor  $g_{ij}$  and Riemannian connection  $\Gamma_{ik}^m$  are required.

In  $d$ -dimensional input space, the decision boundary is generally a  $(d-1)$ -dimensional manifold. We use  $x_i, (i = 1, 2, \dots, d-1)$  as the parameters of decision boundary, thus a point on the boundary is represented as  $\mathbf{r} = (x_1, x_2, \dots, x_{d-1}, x_d)^T$ , where  $x_d = x_d(x_1, x_2, \dots, x_{d-1})$  is implicitly determined by the equation  $f(x_1, x_2, \dots, x_{d-1}, x_d) = 0$  of decision boundary. The metric tensor  $g_{ij}$  is defined by  $ds^2 = \sum_{i,j=1}^{d-1} g_{ij} dx_i dx_j$ . Therefore, by

$$ds^2 = d\mathbf{r} \cdot d\mathbf{r} = dx_1^2 + dx_2^2 + \dots + dx_d^2 = dx_1^2 + dx_2^2 + \dots + dx_{d-1}^2 + \left( \sum_{i=1}^{d-1} \frac{\partial x_d}{\partial x_i} dx_i \right)^2,$$

and by  $\frac{\partial x_d}{\partial x_i} = -f_i/f_d$ , there is  $ds^2 = \sum_{i=1}^{d-1} dx_i^2 + \sum_{i,j=1}^{d-1} \frac{f_i f_j}{f_d^2} dx_i dx_j$ . We get the components of  $g_{ij}$  as follows,

$$\begin{aligned} g_{ii} &= 1 + f_i^2/f_d^2, \quad i = 1, 2, \dots, d-1, \\ g_{ij} &= f_i f_j / f_d^2, \quad i, j = 1, 2, \dots, d-1, \text{ and } i \neq j. \end{aligned} \quad (10)$$

Having metric tensor  $g = (g_{ij})$ , we can compute the Riemannian connection defined as

$$\Gamma_{ik}^m := \frac{1}{2} \Sigma_j g^{mj} (\partial_k g_{ij} + \partial_i g_{kj} - \partial_j g_{ik}),$$

where  $g^{mi}$  is the element of  $g^{-1}$ . The computation is very lengthy and tedious, hence we only show the key techniques to save space. For example,  $\partial_k g_{ij}$  is computed as follows,

$$\begin{aligned} \partial_k g_{ij} &= \frac{\left[ \left( f_{ik} + f_{id} \cdot \frac{\partial x_d}{\partial x_k} \right) f_j + f_i \left( f_{jk} + f_{jd} \frac{\partial x_d}{\partial x_k} \right) \right] f_d^2 - f_i f_j \cdot \left[ 2f_d \left( f_{dk} + f_{dd} \frac{\partial x_d}{\partial x_k} \right) \right]}{f_d^4} \\ &= \frac{f_j f_d^2 f_{ik} + f_i f_d^2 f_{jk} - f_j f_k f_d f_{id} - f_i f_k f_d f_{jd} - 2f_i f_j f_d f_{dk} + 2f_i f_j f_k f_{dd}}{f_d^4}, \quad (i \neq j), \\ \partial_k g_{ii} &= \frac{2f_i f_d^2 f_{ik} - 2f_i f_k f_d f_{id} + 2f_i^2 f_k f_{dd} - 2f_i^2 f_d f_{dk}}{f_d^4}. \end{aligned} \quad (11)$$

The Riemann curvature tensor is defined by

$$R_{bik}^a = \Gamma_{kb,i}^a - \Gamma_{ib,k}^a + \sum_c \Gamma_{ic}^a \Gamma_{kb}^c - \sum_c \Gamma_{kc}^a \Gamma_{ib}^c. \quad (12)$$

The key computation here is  $\Gamma_{kb,i}^a = \frac{\partial \Gamma_{kb}^a}{\partial x_i}$ , which involves the computation of  $\frac{\partial g^{mj}}{\partial x_i}$ . By  $\Sigma_j g^{mj} g_{jn} = \delta_n^m$ , differentiating it gives

$$\Sigma_j \left( \frac{\partial g^{mj}}{\partial x_i} g_{jn} + g^{mj} \frac{\partial g_{jn}}{\partial x_i} \right) = 0.$$

Rewrite in matrix form,

$$\frac{\partial g^{-1}}{\partial x_i} g = -g^{-1} \frac{\partial g}{\partial x_i}.$$

Therefore,

$$\frac{\partial g^{mj}}{\partial x_i} = - \sum_{k,n} g^{mk} \frac{\partial g_{kn}}{\partial x_i} g^{nj}. \quad (13)$$

Finally, the curvature 2-form is

$$\Omega_{ab} = \frac{1}{2} \sum_{i,k} R_{abik} dx^i \wedge dx^k = \frac{1}{2} \sum_{i,k,n} g_{an} R_{bik}^n dx^i \wedge dx^k. \quad (14)$$

$\Omega_{ab}$  will be used in Gauss-Bonnet-Chern theorem to compute Euler characteristics of closed manifolds.

#### 7.4 Proof of Theorem 4.1

For a closed decision boundary curve  $C$  with counter-clockwise positive direction, the rotation index theorem states

$$\frac{1}{2\pi} \int_C k_r ds = 1. \quad (15)$$

We have computed  $k_r$  in (2). Note that  $ds = \sqrt{1 + y'^2} dx = \sqrt{1 + f_x^2/f_y^2} dx$ , we obtain

$$\frac{1}{2\pi} \int_C k_r \sqrt{1 + f_x^2/f_y^2} dx = 1 \quad (16)$$

Using Green's theorem, (16) leads to  $-\frac{1}{2\pi} \iint_{D_1} \frac{\partial(k_r \sqrt{1 + f_x^2/f_y^2})}{\partial y} dx dy = 1$ , where  $D_1$  is the region surrounded by  $C$ . However, since  $C$  is an implicit curve and usually can not be solved analytically, it is hard to get an analytical expression of  $D_1$ . Our key observation here is that inside  $D_1$  (without loss of generality, assume  $D_1$  is the decision region of positive class), the outputs of neural networks satisfy  $f(x, y) > 0$ , and outside  $D_1$  satisfy  $f(x, y) < 0$ . Therefore, we can expand the integral domain from  $D_1$  to the whole definition domain  $D$  as follows,

$$I_{2d} := -\frac{1}{2\pi} \iint_D \text{sgn}(f(x, y)) \frac{\partial(k_r \sqrt{1 + f_x^2/f_y^2})}{\partial y} dx dy = 1 \quad (17)$$

Only region  $D_1$  contributes to the above integral, thus avoiding the difficulty of solving  $D_1$  explicitly. (17) holds for any closed decision boundary curves in 2d input space.

On the other hand, if the decision boundary is open, we are going to prove that (17) does not hold anymore. Suppose decision boundary curve  $C$  is open, it will intersect with boundary of  $D$ , thus as shown in fig.3 we can add a line segment  $L$  on the boundary of  $D$  to make  $C + L$  closed. Then,

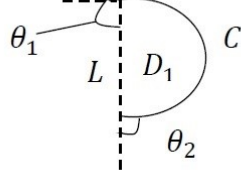


Figure 3: Add a line segment  $L$  to the open decision boundary  $C$  to form a closed region  $D_1$ .

$$\begin{aligned}
 I_{2d} &= -\frac{1}{2\pi} \iint_D \operatorname{sgn}(f(x, y)) \frac{\partial(k_r \sqrt{1+f_x^2/f_y^2})}{\partial y} dx dy \\
 &= -\frac{1}{2\pi} \iint_{D_1} \frac{\partial(k_r \sqrt{1+f_x^2/f_y^2})}{\partial y} dx dy = \frac{1}{2\pi} \int_{C+L} k_r \sqrt{1+f_x^2/f_y^2} dx
 \end{aligned} \tag{18}$$

Here we have used Green's theorem for the piecewise smooth curve  $C + L$ . By assumption 4.1,  $L$  is linear, hence  $k_r = 0$  on  $L$ , which implies

$$\frac{1}{2\pi} \int_{C+L} k_r \sqrt{1+f_x^2/f_y^2} dx = \frac{1}{2\pi} \int_C k_r \sqrt{1+f_x^2/f_y^2} dx = \frac{1}{2\pi} \int_C k_r ds. \tag{19}$$

The rotation index theorem for closed piecewise smooth curves states

$$\int_{C+L} k_r ds + \theta_1 + \theta_2 = 2\pi,$$

where  $\theta_1, \theta_2$  are the angles shown in fig.3. Using the fact  $k_r = 0$  on  $L$  again, we arrive at

$$\frac{1}{2\pi} \int_C k_r ds = 1 - \frac{\theta_1 + \theta_2}{2\pi} \tag{20}$$

Combining (18),(19) and (20), for open decision region there is

$$I_{2d} = 1 - \frac{\theta_1 + \theta_2}{2\pi} \neq 1. \tag{21}$$

Putting (17) and (21) together, we can use index  $I_{2d}$  to judge whether a decision boundary curve is closed.

If decision region  $D_1$  intersects with boundary of  $D$  at multiple line segments along different axes, then  $L$  is composed of multiple linear pieces and each has  $k_r = 0$ . Therefore, the above results still hold.

## 7.5 Proof of Theorem 4.2

From theorem 4.1, for each closed component  $D_i$  of the decision boundary that satisfies  $f(x, y) > 0, (x, y) \in D_i$ , we have  $-\frac{1}{2\pi} \iint_{D_i} \frac{\partial(k_r \sqrt{1+f_x^2/f_y^2})}{\partial y} dx dy = 1$ .

Suppose there are  $n$  such components, then

$$I_{2d} = \sum_{i=1}^n -\frac{1}{2\pi} \iint_{D_i} \frac{\partial \left( k_r \sqrt{1 + f_x^2/f_y^2} \right)}{\partial y} dx dy = n.$$

If  $I_{2d} = n$  (a positive interger), the only possible case is that there are  $n$  closed components in the decision boundary.

On the contrary, if  $I_{2d} \neq n$ , there must be some open components as implied by theorem 4.1.

## 7.6 Proof of Theorem 4.3

For a closed decision surface  $S$ , the Gauss-Bonnet theorem states

$$\iint_S K d\sigma = 2\pi\chi(S), \quad (22)$$

where  $K$  is the Gaussian curvature given in (4),  $\chi(S)$  is the Euler characteristic of  $S$  and takes a value in  $\{2, 0, -2, \dots, -2n, \dots\}$ .  $d\sigma$  is the area element,

$$\begin{aligned} d\sigma &= \sqrt{EG - F^2} dx dy = \sqrt{(1 + f_x^2/f_z^2)(1 + f_y^2/f_z^2) - f_x^2 f_y^2 / f_z^4} dx dy \\ &= \frac{\sqrt{f_x^2 + f_y^2 + f_z^2}}{f_z} dx dy. \end{aligned} \quad (23)$$

For closed surfaces, (22) and (23) yield

$$\iint_S K \frac{\sqrt{f_x^2 + f_y^2 + f_z^2}}{f_z} dx dy = 2\pi\chi(S). \quad (24)$$

Using Gauss's theorem, we get

$$\iiint_{\Omega} \frac{\partial(K \sqrt{f_x^2 + f_y^2 + f_z^2}/f_z)}{\partial z} dV = 2\pi\chi(S), \quad (25)$$

where  $\Omega$  is the 3d region enclosed by  $S$ . Like in the 2d case, it is not necessary to solve  $S$  and  $\Omega$  explicitly, which itself is a difficult task for DNNs. We avoid solving  $\Omega$  by expanding it to the whole definition domain  $D$ ,

$$I_{3d} := \iiint_D \text{sgn}(f(x, y, z)) \frac{\partial(K \sqrt{f_x^2 + f_y^2 + f_z^2}/f_z)}{\partial z} dV = 2\pi\chi(S). \quad (26)$$

On the other hand, we will show that (26) does not hold for open surfaces. If  $S$  is open, we can add a planar surface  $T$  to make  $S + T$  closed, where  $T$  is located on the boundary of  $D$  as illustrated in fig. 4. Then, by Gauss-Bonnet

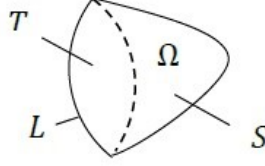


Figure 4: Add a planar surface  $T$  to an open decision surface  $S$ , then  $S + T$  will be closed.

theorem for open surfaces, we have

$$\int_L k_g(s)ds + \iint_S Kd\sigma = 2\pi, \quad (27)$$

where  $L$  is the boundary curve of  $S$ ,  $k_g$  is the geodesic curvature on  $L$ . Therefore, using Gauss's theorem again, we obtain

$$\begin{aligned} I_{3d} &= \iiint_{\Omega} \frac{\partial \left( K \sqrt{f_x^2 + f_y^2 + f_z^2/f_z} \right)}{\partial z} dV \\ &= \iint_{S+T} K \frac{\sqrt{f_x^2 + f_y^2 + f_z^2}}{f_z} dx dy = \iint_{S+T} K d\sigma. \end{aligned}$$

Since  $K = 0$  on planar surface  $T$ , combining with (27), for open surface  $S$  we have

$$I_{3d} = \iint_S K d\sigma = 2\pi - \int_L k_g(s)ds \neq 2\pi. \quad (28)$$

Therefore,  $I_{3d} \neq 2\pi\chi$  when  $\chi \in \{2, 0, -2, -4, \dots\}$ . As a result, whether  $I_{3d} = 2\pi\chi$  holds can be used to determine the openness of decision surfaces.

If decision region  $\Omega$  intersects with boundary of  $D$  at multiple linear pieces, the conclusion above still holds.

## 7.7 Proof of Theorem 4.4

If a decision boundary  $S$  has several components, then by theorem 4.3, each closed component  $S_i$  satisfies  $\iiint_{D_i} \frac{\partial \left( K \sqrt{f_x^2 + f_y^2 + f_z^2/f_z} \right)}{\partial z} dV = 2\pi\chi(S_i)$ , where  $D_i$  is the region surrounded by  $S_i$ . For each open component  $S_j$ , by (27) we have (using  $K = 0$  on  $T$ )

$$\iiint_{D_j} \frac{\partial \left( K \sqrt{f_x^2 + f_y^2 + f_z^2/f_z} \right)}{\partial z} dV = 2\pi - \int_L k_g(s)ds.$$

Therefore,

$$\begin{aligned}
I_{3d} &= \sum_i \iiint_{D_i} \frac{\partial \left( K \sqrt{f_x^2 + f_y^2 + f_z^2} / f_z \right)}{\partial z} dV + \sum_j \iiint_{D_j} \frac{\partial \left( K \sqrt{f_x^2 + f_y^2 + f_z^2} / f_z \right)}{\partial z} dV \\
&= 2\pi \sum_i \chi(S_i) + \sum_j \left( 2\pi - \int_L k_g(s) ds \right).
\end{aligned} \tag{29}$$

If  $I_{3d} = 2\pi\chi$  and  $\chi$  is even, the only possible explanation is that all components are closed. If  $\frac{I_{3d}}{2\pi} = 2n$  ( $n$  is a positive integer and  $n \geq 2$ ), (29) implies  $\sum_i \chi(S_i) = 2n$  ( $n \geq 2$ ), and there must be at least two sphere-like components since  $\chi = 2$  for spheres and  $\chi \leq 0$  for other topological surfaces.

If  $S$  is closed and has a single component, it is straightforward from (26) that  $\chi(S) = \frac{I_{3d}}{2\pi}$ .

## 7.8 Proof of Theorem 4.5

By high-dimensional Gauss-Bonnet-Chern theorem, there is  $\chi(M) = \int_M e(M)$ . Using Stokes' theorem for manifold:  $\int_M e(M) = \int_\Omega de$ , where  $\Omega$  is the volume enclosed by  $M$ , (7) is obtained immediately.

## 7.9 Proof of Theorem 5.1

The output of the  $l$ th layer is  $\mathbf{O}_l = \sigma(\mathbf{W}^l \mathbf{O}_{l-1} + \mathbf{b}^l)$ . Suppose in the  $d$ -dimensional input space, there is a  $(d-1)$ -dimensional closed boundary. If  $d_l < d$ , the affine transformation by  $\mathbf{W}^l$  will collapse the closed boundary, which is irrecoverable in subsequent layers. In other words, some neighboring regions inside and outside the boundary (i.e.,  $f(\mathbf{x}) > 0$  and  $f(\mathbf{x}) < 0$  respectively) will get overlapped after this affine transformation. Therefore, we must have  $d_l \geq d$  in order to produce closed boundaries.

On the other hand, if  $d_L = d$ , suppose after affine transformations of  $(\mathbf{W}^l)_{l=1}^L$  the decision boundary is not collapsed, then  $\sigma(\mathbf{W}^L \mathbf{O}_{L-1} + \mathbf{b}^L)$  will output a  $(d-1)$ -dimensional closed boundary since  $\sigma$  is continuous and bijective. However, this contradicts the fact that the decision boundary is on a  $(d_L - 1)$ -dimensional hyperplane due to  $\mathbf{a}^T \mathbf{O}_L + c = 0$  caused by  $f(\mathbf{x}) = 0$ . Therefore,  $d_L$  must be greater than  $d$ .

## 7.10 Proof of Theorem 6.1

For one-hidden-layer network  $f(\mathbf{x}) = \mathbf{a}^T \sigma(\mathbf{W}\mathbf{x} + \mathbf{b}) + c$ , its 1st-order and 2nd-order partial derivatives have been given in (3). By (2), we can obtain the expression of  $k_r$  in terms of network weights. Here we only concern the following

part of  $k_r$  that will cause  $k_r = 0$ .

$$\begin{aligned}
& f_{xx}f_y^2 - 2f_xf_yf_{xy} + f_x^2f_{yy} \\
&= \sum_{i,j,k} [\mathbf{a}_i\sigma_i''W_{i1}^2 \cdot \mathbf{a}_j\sigma_j'W_{j2} \cdot \mathbf{a}_k\sigma_k'W_{k2} - 2\mathbf{a}_i\sigma_i''W_{i1}W_{i2} \cdot \mathbf{a}_j\sigma_j'W_{j1} \cdot \mathbf{a}_k\sigma_k'W_{k2} \\
&\quad + \mathbf{a}_i\sigma_i''W_{i2}^2 \cdot \mathbf{a}_j\sigma_j'W_{j1}\mathbf{a}_k\sigma_k'W_{k1}] \\
&= \sum_{i,j,k} \sigma_i''\sigma_j'\sigma_k' \cdot \mathbf{a}_i\mathbf{a}_j\mathbf{a}_k \cdot [W_{i1}W_{k2}(W_{i1}W_{j2} - W_{i2}W_{j1}) \\
&\quad + W_{i2}W_{j1}(W_{i2}W_{k1} - W_{i1}W_{k2})] = 0,
\end{aligned} \tag{30}$$

where  $\sigma_i''$  denotes  $\sigma''(\mathbf{w}_i \cdot \mathbf{x} + b_i)$ . For general activation functions such as sigmoid etc.,  $\sigma''(y)$  and  $\sigma'(y)$  can not be zero everywhere. Therefore by (30),  $k_r(\mathbf{x}) = 0$  at any  $\mathbf{x}$  on the decision boundary requires

$$\begin{aligned}
\mathbf{a}_i\mathbf{a}_j\mathbf{a}_k [W_{i1}W_{k2}(W_{i1}W_{j2} - W_{i2}W_{j1}) + W_{i2}W_{j1}(W_{i2}W_{k1} - W_{i1}W_{k2})] = 0, \\
(i, j, k \in [d_1]).
\end{aligned} \tag{31}$$

There are several possible non-trivial (i.e.,  $\mathbf{a} \neq 0$  and  $W \neq 0$ ) cases making (31) satisfied, which constitute the sufficient conditions for  $k_r(\mathbf{x}) = 0$ .

**a)**  $\mathbf{a}_iW_{i1} = 0$  or  $\mathbf{a}_iW_{i2} = 0$ . So, if  $\mathbf{a}_i \neq 0$ , there is  $W_{i1} = 0$  or  $W_{i2} = 0$ . Let  $I = \{i | \mathbf{a}_i \neq 0\}$ , we have (assume  $\mathbf{a}_iW_{i1} = 0$ )

$$f(\mathbf{x}) = \sum_{i \in I} a_i \sigma(W_{i2}y + b_i) + c = 0$$

due to  $W_{i1} = 0, (i \in I)$ . This equation only involves variable  $y$ . As a result, its solution  $y^*$  determines a linear decision boundary parallel to  $x$  axis.

**b)**  $\mathbf{a}_i\mathbf{a}_j(W_{i1}W_{j2} - W_{i2}W_{j1}) = 0$ .  $W_{i1}W_{j2} - W_{i2}W_{j1} = 0$  means the  $i$ th row and  $j$ th row of  $W$  are linear dependent. With loss of generality, suppose  $\mathbf{w}_1, \mathbf{w}_2, \dots, \mathbf{w}_k$  ( $k \leq d_1, \{1, 2, \dots, k\} \in I, \mathbf{w}_1 \neq 0$ ) are linear dependent, thus  $\mathbf{w}_i = c_i\mathbf{w}_1$  ( $i \in [k], c_i$  is a constant). Then,

$$f(\mathbf{x}) = \sum_{i \in I} a_i \sigma(c_i\mathbf{w}_1 \cdot \mathbf{x} + b_i) + c = 0.$$

$f(\mathbf{x})$  now only involves  $\mathbf{w}_1 \cdot \mathbf{x}$ . By solving  $g(\mathbf{w}_1 \cdot \mathbf{x}) := f(\mathbf{x}) = 0$ , the solution  $\mathbf{w}_1 \cdot \mathbf{x} = d^*$  produces a linear decision boundary in input space whose normal is  $\mathbf{w}_1$ .

A special case is that  $\mathbf{a}$  is a one-hot vector, i.e., only one component of  $\mathbf{a}$  is non-zero. Without loss of generality, assume  $\mathbf{a}_i \neq 0$ . When  $i = j = k$ , (31) is satisfied and thus  $k_r = 0$ . Geometrically,  $f(\mathbf{x}) = a_i \sigma(\mathbf{w}_i \cdot \mathbf{x} + b_i) + c = 0$  leads to  $\mathbf{w}_i \cdot \mathbf{x} + b_i - \sigma^{-1}\left(-\frac{c}{a_i}\right) = 0$ , which is an equation of line. Therefore, one-hot vector  $\mathbf{a}$  yields a linear decision boundary with normal  $\mathbf{w}_i$ .

## 7.11 Proof of Theorem 6.2

The derivatives of  $f(\mathbf{x}) = \mathbf{a}^T \sigma(U\sigma(V\mathbf{x} + \mathbf{b}_1) + \mathbf{b}_2) + c$  are as follows,

$$\begin{aligned} f_x &= \sum_{i,j} \mathbf{a}_i \sigma'_{2ij} U_{ij} \sigma'_{1j} V_{j1}, & f_y &= \sum_{i,j} \mathbf{a}_i \sigma'_{2ij} U_{ij} \sigma'_{1j} V_{j2} \\ f_{xx} &= \sum_{i,j,k} \mathbf{a}_i [\sigma''_{2ij} U_{ij} \sigma'_{1j} V_{j1}] U_{ik} \sigma'_{1k} V_{k1} + \sum_{i,j} \mathbf{a}_i \sigma'_{2ij} U_{ij} \sigma''_{1j} V_{j1}^2, \end{aligned}$$

where  $\sigma'_{2ij}$  denotes  $\sigma'(U_{ij}\sigma(\mathbf{v}_j \cdot \mathbf{x} + \mathbf{b}_{1,j}) + \mathbf{b}_{2,i})$ , and  $\sigma'_{1j} = \sigma'(\mathbf{v}_j \cdot \mathbf{x} + \mathbf{b}_{1,j})$ .  $f_{xx}$  and  $f_{yy}$  can be obtain similarly. After careful arrangement, we get

$$\begin{aligned} f_{xx} f_y^2 - 2f_{xy} f_x f_y + f_{yy} f_x^2 &= \\ \sum_{i,j,p,l,m,n} \mathbf{a}_i \mathbf{a}_p \mathbf{a}_m &\left[ \sum_k \sigma''_{2ij} \sigma'_{1j} \sigma'_{1k} \sigma'_{2pl} \sigma'_{1l} \sigma'_{2mn} \sigma'_{1n} \cdot U_{ij} U_{ik} U_{pl} U_{mn} \right. \\ & (V_{j1} V_{k1} V_{l2} V_{n2} - 2V_{j2} V_{k1} V_{l1} V_{n2} + V_{j2} V_{k2} V_{l1} V_{n1}) + \sigma'_{2ij} \sigma''_{1j} \sigma'_{2pl} \sigma'_{1l} \sigma'_{2mn} \sigma'_{1n} \\ & \left. U_{ij} U_{pl} U_{mn} (V_{j1}^2 V_{l2} V_{n2} - 2V_{j1} V_{j2} V_{l1} V_{n2} + V_{j2}^2 V_{l1} V_{n1}) \right] = 0. \end{aligned}$$

Because we require  $k_r = 0$  at all points on the decision boundary, by the fact that  $\sigma''_{2ij}$  and  $\sigma'_{1j}$  etc. cannot be zero everywhere, the following must be satisfied,

$$\begin{aligned} \mathbf{a}_i \mathbf{a}_p \mathbf{a}_m \cdot U_{ij} U_{ik} U_{pl} U_{mn} [V_{k1} V_{n2} (V_{j1} V_{l2} - V_{j2} V_{l1}) + V_{j2} V_{l1} (V_{k2} V_{n1} - V_{k1} V_{n2})] \\ = 0, \quad (i, p, m \in [d_2], j, k, l, n \in [d_1]), \end{aligned} \tag{32}$$

and

$$\begin{aligned} \mathbf{a}_i \mathbf{a}_p \mathbf{a}_m \cdot U_{ij} U_{pl} U_{mn} [V_{j1} V_{n2} (V_{j1} V_{l2} - V_{j2} V_{l1}) + V_{j2} V_{l1} (V_{j2} V_{n1} - V_{j1} V_{n2})] \\ = 0, \quad (i, p, m \in [d_2], j, l, n \in [d_1]). \end{aligned} \tag{33}$$

Discarding the trivial solutions  $\mathbf{a} = 0, U = 0$  and  $V = 0$ , the following conditions are sufficient for  $k_r = 0$ .

**a)**  $V_{\cdot,1} = 0$  or  $V_{\cdot,2} = 0$  or  $V_{j1} V_{l2} - V_{j2} V_{l1} = 0$  ( $\forall j, l \in [d_1]$ ).

If  $V_{\cdot,1} = 0$  or  $V_{\cdot,2} = 0$ , the image of  $V\mathbf{x} + \mathbf{b}_1$  is a line, so the image of  $\sigma(U\sigma(V\mathbf{x} + \mathbf{b}_1) + \mathbf{b}_2)$  becomes a curve which intersects the hyperplane determined by  $\mathbf{a}$  and  $c$  at a point. The pre-image of this intersection point in input space is a line parallel to  $x$  or  $y$  axis for  $V_{\cdot,1} = 0$  or  $V_{\cdot,2} = 0$  respectively.

If  $V_{j1} V_{l2} - V_{j2} V_{l1} = 0$  ( $\forall j, l \in [d_1]$ ), the image of  $V\mathbf{x} + \mathbf{b}_1$  is then again a line, and similarly the decision boundary is a line.

The above cases concern only weight  $V$  of the first hidden layer, which transforms the 2d input space into a line. However, the weights  $U, V$  and  $\mathbf{a}$  in different layers can work together to produce linear decision boundaries and the image of  $V\mathbf{x} + \mathbf{b}_1$  needs not to be a line, as demonstrated by the following case.

**b)** For  $i \in [d_2]$  and  $j, l \in [d_1]$ ,

$$\mathbf{a}_i U_{ij} V_{j1} = 0 \text{ or } \mathbf{a}_i U_{ij} V_{j2} = 0 \text{ or } \mathbf{a}_i U_{ij} (V_{j1} V_{l2} - V_{j2} V_{l1}) = 0.$$



If  $a_i U_{ij} V_{j1} = 0$ , let  $I = \{i | a_i \neq 0\}$ ,  $J = \{j | U_{ij} \neq 0\}$ , then  $V_{j1} = 0$  ( $i \in I, j \in J$ ). We have

$$f(\mathbf{x}) = \sum_{i \in I} a_i \sigma \left( \sum_{j \in J} U_{ij} \sigma (V_{j2} y + b_{1,j}) + b_{2,i} \right) + c = 0$$

This equation involves only variable  $y$ , thus producing a linear decision boundary parallel to  $x$  axis.

If  $a_i U_{ij} (V_{j1} V_{l2} - V_{j2} V_{l1}) = 0$ , there is  $V_{j1} V_{l2} - V_{j2} V_{l1} = 0$  ( $i \in I; j \in J; l \in [d_1]$ ). Hence  $V$  is a rank-deficient matrix, and without loss of generality there is  $\mathbf{v}_l = c_l \mathbf{v}_1$  ( $\mathbf{v}_1 \neq 0$ ). Therefore,

$$f(\mathbf{x}) = \sum_{i \in I} a_i \sigma \left( \sum_{j \in J} U_{ij} \sigma (c_j \mathbf{v}_1 \cdot \mathbf{x} + b_{1,j}) + b_{2,i} \right) + c = 0$$

This is an equation of  $\mathbf{v}_1 \cdot \mathbf{x}$ , generating a linear decision boundary in 2d input space whose normal is  $\mathbf{v}_1$ .

## 7.12 Proof of Theorem 6.3

Given the derivatives for one-hidden-layer networks, the numerator of  $K$  in (4) can be expressed as

$$\begin{aligned} & (2f_{xz}f_xf_z - f_{xx}f_z^2 - f_{zz}f_x^2)(2f_{yz}f_yf_z - f_{yy}f_z^2 - f_{zz}f_y^2) \\ & - (f_{yz}f_xf_z + f_{xz}f_yf_z - f_{zz}f_xf_y - f_{xy}f_z^2)^2 \\ & = \sum_{i,j,k,l,m,n} a_i a_j a_k a_l a_m a_n \sigma''_i \sigma'_j \sigma'_k \sigma''_l \sigma'_m \sigma'_n \{ [W_{i1}W_{k3}(W_{i3}W_{j1} - W_{i1}W_{j3}) \\ & + W_{i3}W_{j1}(W_{i1}W_{k3} - W_{i3}W_{k1})] [W_{l2}W_{n3}(W_{l3}W_{m2} - W_{l2}W_{m3}) \\ & + W_{l3}W_{m2}(W_{l2}W_{n3} - W_{l3}W_{n2})] \\ & - [W_{i3}W_{j1}(W_{i2}W_{k3} - W_{i3}W_{k2}) + W_{i1}W_{k3}(W_{i3}W_{j2} - W_{i2}W_{j3})] \\ & \cdot [W_{l3}W_{m1}(W_{l2}W_{n3} - W_{l3}W_{n2}) + W_{l1}W_{n3}(W_{l3}W_{m2} - W_{l2}W_{m3})] \} = 0. \end{aligned} \tag{34}$$

The following conditions are sufficient to make (34) satisfied: for  $i, j, k \in [d_1]$ ,

$$\begin{aligned} & a_i a_j a_k [W_{i1}W_{k3}(W_{i3}W_{j1} - W_{i1}W_{j3}) + W_{i3}W_{j1}(W_{i1}W_{k3} - W_{i3}W_{k1})] = 0 \\ & \text{or } a_i a_j a_k [W_{i2}W_{k3}(W_{i3}W_{j2} - W_{i2}W_{j3}) + W_{i3}W_{j2}(W_{i2}W_{k3} - W_{i3}W_{k2})] = 0, \\ & \text{and } a_i a_j a_k [W_{i3}W_{j1}(W_{i2}W_{k3} - W_{i3}W_{k2}) + W_{i1}W_{k3}(W_{i3}W_{j2} - W_{i2}W_{j3})] = 0, \end{aligned} \tag{35}$$

which further lead to the following sufficient conditions for  $K = 0$ .

**a)**  $a_i W_{i1} = 0$  or  $a_i W_{i2} = 0$  or  $a_i W_{i3} = 0, (\forall i \in [d_1])$ . As an example,  $a_i W_{i1} = 0$  means  $W_{i1} = 0$  ( $i \in I$ ). Thus, on the decision boundary,

$$f(\mathbf{x}) = \sum_{i \in I} a_i \sigma (W_{i2} y + W_{i3} z + b_i) + c = 0.$$

This is an equation of  $y$  and  $z$ , giving an implicit curve  $z = z(y)$ . The pre-image of this curve in 3d input space is a developable surface that is straight along  $x$  direction.

**b)**  $a_i a_j (W_{i3}W_{j2} - W_{i2}W_{j3}) = 0, (\forall i, j \in [d_1])$ . This case also generates developable decision boundaries. The reason is as follows. We have

$$f(\mathbf{x}) = \sum_{i \in I} a_i \sigma(W_{i1}x + W_{i2}y + W_{i3}z + b_i) + c = 0.$$

Choose an index  $k$  for which  $a_k \neq 0$ , then  $W_{i3}W_{j2} - W_{i2}W_{j3} = 0$  implies  $\mathbf{w}_{j,2\sim 3} = c_j \mathbf{w}_{k,2\sim 3}, (j \in I)$ , where  $\mathbf{w}_{j,2\sim 3}$  denotes the vector composed of the 2nd and 3rd columns of  $\mathbf{w}_j$ . Define a new variable  $y' = W_{k2}y + W_{k3}z$ , then

$$f(\mathbf{x}) = \sum_{i \in I} a_i \sigma(W_{i1}x + c_i y' + b_i) + c = 0.$$

This is an equation of  $x$  and  $y'$  whose solution is  $y' = y'(x)$ . Therefore, for any value of  $x$ , we have

$$W_{k2}y + W_{k3}z = y'(x),$$

which specifies a line parallel to  $y - z$  plane with normal  $(0, W_{k2}, W_{k3})^\top$ . The whole decision boundary is a developable surface. One-hot vector  $\mathbf{a}$  is a special case. Suppose  $a_i \neq 0$ , (35) holds automatically when  $i = j = k$ . This results in a linear decision boundary with normal  $\mathbf{w}_i$ .

### 7.13 Proof of Theorem 6.4

The condition  $a_i W_{ij}^L W_{jk}^{L-1} \dots W_{mn}^2 = 0$  makes the term  $\sigma(\mathbf{w}_n^1 \cdot \mathbf{x} + \mathbf{b}^1)$  vanishing in  $f(\mathbf{x})$ , thus  $f(\mathbf{x}) = 0$  only involves  $\mathbf{w}_l^1 \cdot \mathbf{x} (l \neq n)$ . Linear dependency among  $\mathbf{w}_l^1 (l \neq n)$  will give a linear decision boundary with normal  $\mathbf{w}_l^1$  (any  $l \neq n$ ).

When  $W_{lq}^1 = 0 (l \neq n)$ ,  $x_q$  will disappear in equation  $f(\mathbf{x}) = 0$ , and the solution to  $f(x_1, x_2, \dots, x_{q-1}, x_{q+1} \dots x_d) = 0$  is an implicit hypersurface which is straight along  $x_q$ . This conclusion holds when the cardinality of  $q$  is greater than 1, i.e., the decision boundary is straight along several axes.

## 8 Conclusion and future work

We have computed the curvatures of decision boundaries produced by DNNs using knowledge of differential geometry. We then proposed methods to identify the closeness and connectivity of given decision boundaries, and obtain the Euler characteristics of closed ones. All these methods are based on particular integrals of curvatures and there are no needs to solve the decision boundaries explicitly. We then proved that in order to produce closed decision boundaries, the last hidden layer must be wider than and all other hidden layers must be wider than

or equal to the input dimension. Finally, we gave sufficient conditions on network weights for producing zero curvature (flat or developable) decision boundaries.

In future work, we plan to apply efficient numerical techniques to calculate the integrals proposed in section 4 for identifying the topological properties of DNNs' decision regions. It is also worthwhile to design homology inspired analytical approaches for scenarios methods in section 4 are unable to deal with (such as the non-uniqueness of number and types of connected components). Finally, we are also interested in analyzing the constraints on network architecture and weights in order to produce decision boundaries with more complex geometrical properties, such as convexity or constant curvatures.

## References

- [1] Serguei Barannikov, Alexander Korotin, Dmitry Oganessian, Daniil Emtsev, and Evgeny Burnaev. Barcodes as summary of objective functions topology. *arXiv preprint arXiv:1912.00043*, 2019.
- [2] Hans-Peter Beise, Steve Dias Da Cruz, and Udo Schrder. On decision regions of narrow deep neural networks. *arXiv preprint arXiv:1807.01194*, 2018.
- [3] M. Bianchini and F. Scarselli. On the complexity of neural network classifiers: A comparison between shallow and deep architectures. *IEEE Transactions on Neural Networks and Learning Systems*, 25(8):15531565, 2014.
- [4] Manfredo P. Do Carmo. *Differential Geometry of Curves and Surfaces, 1st edition*. Prentice-Hall, 1976.
- [5] Chao Chen, Xiuyan Ni, Qinxun Bai, and Yusu Wang. A topological regularizer for classifiers via persistent homology. In *AISTATS*, 2019.
- [6] Tian Ding, Dawei Li, and Ruoyu Sun. Spurious local minima exist for almost all over-parameterized neural networks. *optimization online*, 2019.
- [7] Felix Draxler, Kambis Veschgini, Manfred Salmhofer, and Fred A. Hamprecht. Essentially no barriers in neural network energy landscape. In *International Conference on Machine Learning*, 2018.
- [8] Simon S. Du and Jason D. Lee. On the power of over-parametrization in neural networks with quadratic activation. In *International Conference on Machine Learning*, 2018.
- [9] H Edelsbrunner and J Harer. Persistent homologya survey. *Contemporary Mathematics*, 453:257282, 2008.
- [10] Alhussein Fawzi, Seyed-Mohsen Moosavi-Dezfooli, Pascal Frossard, and Stefano Soatto. Empirical study of the topology and geometry of deep networks. In *IEEE Conference on Computer Vision and Pattern Recognition (CVPR)*, 2018.

- [11] Soheil Feizi, Hamid Javadi, Jesse Zhang, and David Tse. Porcupine neural networks:(almost) all local optima are global. *arXiv preprint arXiv:1710.02196*, 2017.
- [12] C Daniel Freeman and Joan Bruna. Topology and geometry of half-rectified network optimization. In *International Conference on Learning Representations*, 2017.
- [13] Weihao Gao, Ashok Vardhan Makkua, Sewoong Oh, and Pramod Viswanath. Learning one-hiddenlayer neural networks under general input distributions. *arXiv preprint arXiv:1810.04133*, 2018.
- [14] Timur Garipov, Pavel Izmailov, Dmitrii Podoprikin, Dmitry P Vetrov, and Andrew G Wilson. Loss surfaces, mode connectivity, and fast ensembling of dnns. In *Advances in Neural Information Processing Systems*, 2018.
- [15] R. Ge, J. D. Lee, and T. Ma. Learning one-hidden-layer neural networks with landscape design. *arXiv preprint arXiv:1711.00501*, 2017.
- [16] Ian J Goodfellow, Oriol Vinyals, and Andrew M Saxe. Qualitatively characterizing neural network optimization problems. In *International Conference on Learning Representations*, 2015.
- [17] William H. Guss and Ruslan Salakhutdinov. On characterizing the capacity of neural networks using algebraic topology. *arXiv preprint arXiv:1802.04443*, 2018.
- [18] Moritz Hardt and Tengyu Ma. Identity matters in deep learning. In *International Conference on Learning Representations*, 2017.
- [19] Christoph D. Hofer, Roland Kwitt, Mandar Dixit, and Marc Niethammer. Connectivity-optimized representation learning via persistent homology. In *International Conference on Machine Learning*, 2019.
- [20] Y. Jia, E. Shelhamer, J. Donahue, S. Karayev, J. Long, R. Girshick, S. Guadarrama, and T. Darrell. Caffe: Convolutional architecture for fast feature embedding. In *ACM International Conference on Multimedia (MM)*, 2014.
- [21] K. Kawaguchi. Deep learning without poor local minima. In *Advances in Neural Information Processing Systems*, pages 586–594, 2016.
- [22] Kenji Kawaguchi and Leslie Pack Kaelbling. Elimination of all bad local minima in deep learning. *arXiv preprint arXiv:1901.00279*, 2019.
- [23] Thomas Laurent and James H. von Brecht. Deep linear networks with arbitrary loss: All local minima are global. In *International Conference on Machine Learning*, 2018.
- [24] Thomas Laurent and James H. von Brecht. The multilinear structure of relu networks. In *International Conference on Machine Learning*, 2018.

- [25] J. M. Lee. *Manifolds and differential geometry*. American Mathematical Society Providence, 2009.
- [26] Dawei Li, Tian Ding, and Ruoyu Sun. On the benefit of width for neural networks: Disappearance of bad basins. *arXiv preprint arXiv:1812.11039*, 2018.
- [27] Hao Li, Zheng Xu, Gavin Taylor, Christoph Studer, and Tom Goldstein. Visualizing the loss landscape of neural nets. In *Advances in Neural Information Processing Systems*, 2018.
- [28] Shiyu Liang, Ruoyu Sun, Jason D. Lee, and R. Srikant. Adding one neuron can eliminate all bad local minima. In *Advances in Neural Information Processing Systems*, 2018.
- [29] Shiyu Liang, Ruoyu Sun, Yixuan Li, and R. Srikant. Understanding the loss surface of neural networks for binary classification. In *International Conference on Machine Learning*, 2018.
- [30] Qianli Liao and Tomaso Poggio. Theory of deep learning ii: Landscape of the empirical risk in deep learning. *arXiv preprint arXiv:1703.09833*, 2017.
- [31] Bo Liu. Understanding global loss landscape of one-hidden-layer relu neural networks. *arXiv preprint arXiv:2002.04763*, 2020.
- [32] Haihao Lu and Kenji Kawaguchi. Depth creates no bad local minima. *arXiv preprint arXiv:1702.08580*, 2017.
- [33] Seyed-Mohsen Moosavi-Dezfooli, Alhussein Fawzi, Jonathan Uesato, and Pascal Frossard. Robustness via curvature regularization, and vice versa. In *IEEE Conference on Computer Vision and Pattern Recognition (CVPR)*, 2019.
- [34] Q. Nguyen and M. Hein. On connected sublevel sets in deep learning. In *International Conference on Machine Learning*, 2019.
- [35] Q. Nguyen, M. Mukkamala, and M. Hein. Neural networks should be wide enough to learn disconnected decision regions. In *International Conference on Machine Learning*, 2018.
- [36] Quynh Nguyen, Mahesh Chandra Mukkamala, and Matthias Hein. On the loss landscape of a class of deep neural networks with no bad local valleys. In *International Conference on Learning Representations*, 2019.
- [37] Maher Nouiehed and Meisam Razaviyayn. Learning deep models: Critical points and local openness. *arXiv preprint arXiv:1803.02968*, 2018.
- [38] Ben Poole, Subhaneil Lahiri, Maithra Raghu, Jascha Sohl-Dickstein, and Surya Ganguli. Exponential expressivity in deep neural networks through transient chaos. In *Advances in Neural Information Processing Systems*, 2016.

- [39] Karthikeyan Natesan Ramamurthy, Kush R. Varshney, and Krishnan Mody. Topological data analysis of decision boundaries with application to model selection. In *International Conference on Machine Learning*, 2019.
- [40] I. Safran and O. Shamir. On the quality of the initial basin in overspecified neural networks. In *International Conference on Machine Learning*, pages 774–782, 2016.
- [41] I. Safran and O. Shamir. Spurious local minima are common in two-layer relu neural networks. In *International Conference on Machine Learning*, 2018.
- [42] M. Soltanolkotabi, A. Javanmard, and J. D. Lee. Theoretical insights into the optimization landscape of overparameterized shallow neural networks. *IEEE Transactions on Information Theory*, 65(2):742–769, 2019.
- [43] D. Soudry and E. Hoffer. Exponentially vanishing suboptimal local minima in multilayer neural networks. In *arXiv preprint*, page arXiv:1702.05777, 2017.
- [44] Grzegorz Swirszcz, Wojciech Marian Czarnecki, and Razvan Pascanu. Local minima in training of deep networks. *arXiv preprint arXiv:1611.06310*, 2016.
- [45] Luca Venturi, Afonso Bandeira, and Joan Bruna. Spurious valleys in two-layer neural network optimization landscapes. *arXiv preprint arXiv:1802.06384*, 2018.
- [46] Chulhee Yun, Suvrit Sra, and Ali Jadbabaie. Global optimality conditions for deep neural networks. In *International Conference on Learning Representations*, 2018.
- [47] Chulhee Yun, Suvrit Sra, and Ali Jadbabaie. Small nonlinearities in activation functions create bad local minima in neural networks. In *International Conference on Learning Representations*, 2019.
- [48] Li Zhang. Depth creates no more spurious local minima. *arXiv preprint arXiv:1901.09827*, 2019.
- [49] Yi Zhou and Yingbin Liang. Critical points of neural networks: Analytical forms and landscape properties. In *International Conference on Learning Representations*, 2018.